https://doi.org/10.1016/j.jhydrol.2021.126462

Title: Bering Sea Marine Heatwaves: Patterns, Trends and Connections with the Arctic

Author names and affiliations: K.S. Carvalho[a], T.E. Smith[b], S. Wang[a*]

[a]Department of Land Surveying and Geo-Informatics, The Hong Kong Polytechnic University, Hong Kong, China

[b]Department of Geology, Lund University, Sölvegatan 12, 223 62 Lund, Sweden

[*]Corresponding author. Phone: (852) 3400-3896; Email: shuo.s.wang@polyu.edu.hk

Abstract

The conterminous marine system of the Bering Sea serves as an important connection between the Pacific and the Arctic. Surface water temperatures of the Northern Pacific have been rising over the past decades with associated changes in extremes: marine heatwaves (MHWs). This study aims to explore the spatiotemporal evolution characteristics and occurrence mechanisms of MHWs in the Bering Sea. Our findings reveal that MHW metrics are above average in most parts of the Bering Sea, with the number of days being more than 50 a year. Frequencies of MHWs are relatively high in the western sectors while durations and intensities are high in the eastern and southern sectors of the Bering Sea. Increasing trends in the MHW days are noticed almost everywhere while similar increases in MHW intensities are found in the northern Bering Sea. In addition, Chukchi Sea ice concentrations show a negative correlation with heatwave frequencies and days while the Arctic Oscillation has no significant connection. Positive correlations are observed between Chukchi sea temperatures and Alaskan air temperatures, implying influences on the MHW frequencies and days. While the annual trends in the MHW frequencies and days peak over several periods, the latest decade (2010–2019) has seen the highest of both. Our findings suggest that the spatiotemporal distribution of MHW metrics is connected with underlying physical processes in the Bering Sea and neighbouring climatic patterns such as the Pacific teleconnections, sea ice extent, air temperature, and its location within the Arctic.

Keywords: Bering Sea; Marine Heatwave; Arctic; Climate Variability; Temperature

1. Introduction

Anthropogenic warming and its consequent climate impacts have been promulgated in recent studies attracting global attention in climate sciences. With continuous research on increasing temperatures, drought frequencies and incessant weather spells, extreme events have become an important subject in climate change research (Jentsch et al., 2007; Wang and Zhu, 2020). One category of extreme events, known as 'heatwaves', has been receiving great attention over the years. Heatwaves are defined as the periods of abnormally hot weather conditions, which have been increasing in frequency and intensity, hampering human health and ecosystems in the recent decades. A similar phenomenon, called 'marine heatwaves' (MHW), has been known to occur in oceans, threatening marine ecosystems and productivity (Selig et al., 2010; Frölicher and Laufkötter, 2018; Smale et al., 2019). This term has also seen updated definitions based on statistical properties and other metrics (Meehl and Tebaldi, 2004; Fischer et al., 2011; Perkins and Alexander, 2013). The latest definition describes MHWs as discrete periods of anomalously warm sea surface temperatures, ranging for days to months and can extend up to thousands of kilometres (Hobday et al., 2016). Notable MHWs have occurred in the Mediterranean Sea (Sparnocchia et al., 2006; Olita et al., 2007), in the Tasman Sea off the coast of Australia (Oliver et al., 2017), in the northwest Atlantic Ocean in 2012 (Mills et al., 2013) and in the North Pacific including the recent "Blob" (Bond et al., 2015; Scannell et al., 2016).

Even with substantial knowledge of global SST changes, an investigation of previous occurrences of MHWs and associated climate processes are still lacking (Frölicher and Laufkötter, 2018). In addition, there is still an ongoing debate on recent Arctic changes in influencing broader hemispheric weather patterns (Francis, 2017; Kretschmer et al., 2018). Previous studies have indicated that large-scale circulation patterns in the Northern Hemisphere are, in some degree, influenced by Arctic amplification (Francis and Vavrus, 2012). On the contrary, there are other studies highlighting an insignificant relationship between Arctic warming and circulation patterns (and waviness) in mid-latitudes where most of the changes occur due to internal variability or thermodynamic effects in particular seasons (Screen, 2014; Blackport and Screen, 2020).

The percentage of sea surface temperature (SST) change is the highest in the high latitudes of the Northern Hemisphere for near-term and future long-term scenarios (Ruela et al., 2020). Such changes occur due to the inter-decadal variability of upper ocean temperatures which are more prominent in the higher northern latitudes as compared to the Tropical oceans (Wang et al., 2010). With marine ecosystems being vulnerable to the consequences of MHWs, there is a need to assess the extent and prevalence of MHWs on regional scales.

The Bering Sea, among other oceans in the Northern Hemisphere is expected to have higher changes in SSTs in the near future (Ruela et al., 2020). The Bering Sea and Chukchi Sea of the Arctic are known to have similar patterns in ocean-atmospheric warming and have been linked to ocean currents and teleconnections of the Pacific (Carvalho and Wang, 2020). Climate variability in the Bering Sea is largely heterogeneous and is influenced not only by seasonal patterns, but also by sea-ice changes, air temperature and other meteorological components which are sensitive to the Arctic cryosphere (Wood et al., 2015). The Pacific Arctic region which encompasses the Bering-Chukchi complex has been linked with ocean heat transport and inflows via the Bering Strait influencing Arctic sea ice and global hydrological circulations (Woodgate et al., 2012). In addition, the anomalous conditions in the Bering Sea (1997-1998), studied by Yeo et al. (2014) indicates no significant relationship of SST, sea ice and energy flux between the Bering and Chukchi Seas. Nevertheless, there is still a lack of studies revolving around extreme climates in the Bering Sea. Hence, a more in-depth outlook is desired to explore the occurrence of MHWs and associated air-sea interactions with the Arctic.

Here, we will investigate different statistical properties including duration, frequency and intensity of MHWs since the late 1990s on spatial and temporal scales. Furthermore, the recorded MHWs over the time period (1990–2019) will be investigated with other climatic variables in the adjoining high latitudes. The MHW annual frequencies and days will be correlated with various variables to decipher possible connections or drivers of MHWs in the Bering Sea (details provided in Section 2.2). Therefore, the objective of this study is to explore the spatiotemporal evolution characteristics and occurrence mechanisms of MHWs in the Bering Sea.

This paper will be organized as follows: Section 2 will introduce data sources and methods involved in exploring MHW characteristics and occurrence mechanisms; Section 3 presents an in-depth analysis of MHW metrics on spatio-temporal scales; Section 4 provides a thorough discussion on the Bering Sea MHW variations and connections with the Arctic climate; Section 5 summarizes the main conclusions drawn from this study.

2. Data and Methods

2.1. Data sources

The standard MHW definition is applied to the National Oceanic and Atmospheric Administration (NOAA) Optimum Interpolation (OI) SST V2 (and V 2.1, available for 2016 onwards) high resolution (1/4°) gridded SST data for the period 1982 to 2019. The time period for studying MHW statistics in the Bering Sea is from 1990 to 2019 (Figure 1). The Bering Sea is bounded by Russia on the north and west, Alaska in the east and the Aleutian

Islands in the south. The Bering Sea occupies a geographic location which is susceptible to various oscillation patterns and seasonal extremes (Niebauer, 1988). It is constrained by latitudes 160°E-150°W and longitudes 53°N-60°N. The daily OISST data is constructed by combining observations from various platforms (satellites, ships and floats) and interpolated on a global grid (Reynolds et al., 2007). The analysis data contains in-situ data as well as the large-scale adjustment and corrections of satellite biases. The new version (V2.1) contains additional significant improvements in Arctic observations as well (Arctic buoys, SST improvements as a function of sea ice) (Banzon et al., 2020). The MHW analysis will be applied to the Bering Sea, providing a more comprehensive outlook of extremes in the mid-high latitudinal sea. (Figure 1).

2.2. Marine heatwave metrics

A marine heatwave is defined as a "discrete and prolonged anomalously warm water event" and is identified from daily SST time series. Each of the terms "discrete", "prolonged" and "anomalously warm" has been qualitatively described in a marine context (Hobday et al., 2016). Explicitly, "discrete" implies an MHW event with distinct start and end dates, "prolonged" represents a clear MHW count which means a persistence of the event for five consecutive days, and "anomalously warm" indicates that the water temperature is above a climatological threshold (defined as the 90th percentile threshold). Hence the climatological threshold is from 1982 to 2012 which is the acceptable time period for determining the threshold (a minimum of 30 years) according to Hobday et al. (2016). The climatological mean and the 90th percentile threshold can be calculated for each day of the year using daily temperatures across all years in each grid. The climatological threshold, once obtained, can be used in the detection of warm and cold spells. Such definitions have also been implemented in software tools such as R (https://github.com/cran/RmarineHeatWaves) and Matlab (https://github.com/ZijieZhaoMMHW/m_mhw1.0). Therefore, MHWs are identified as periods that are above a threshold for at least five consecutive days, and gaps between events of two or less days with a subsequent five day or more MHW events are also considered as continuous events. .

An MHW can be identified at any point in the ocean from the gridded dataset with the aid of a hierarchical set of metrics (Table 1). Metrics including duration and intensity (collectively termed as primary metrics) can be calculated. These properties are defined as follows: “duration” is the time period between a given start and end date, “maximum intensity” is the maximum temperature recorded relative to a climatological threshold over the duration of the respective event, and “cumulative intensity” is the sum of temperature anomalies for the duration of the event. “Mean intensity” is the mean anomalous temperature for the given MHW event. Mean states and trends can also be calculated for each MHW property. “Frequency” is the event counts in each year, and “days” are referred to as the sum of MHW days in each year. Annual time series can be calculated on temporal scales for each MHW metric.

Place Figure 1 here

Place Table 1 here

2.3. Correlation analysis

To understand the Bering Sea-Arctic connections, statistical analyses of MHWs will be carried out. Climate variables will be correlated with the annual frequency and the annual number of days (MHW days) recorded in the Bering Sea. The annual MHW frequencies and days are calculated by averaging the respective values over the entire grid area of the Bering Sea, thereby including MHW events on different spatial scales. The resultant temporal variations are correlated with the following variables: Sea Surface Temperature (SST) and Sea Ice Concentration (SIC) of the Chukchi Sea, Alaskan and Russian Arctic Air Temperatures, the teleconnection pattern, and the Arctic Oscillation (AO). Here, the Russian Arctic is the geographical region of Russia north of 65°N while Alaska is the region in the pan-Arctic containing 13 climate divisions based on vegetation types, climate and extreme events (Bieniek et al., 2011; Smith et al., 2014). The Chukchi Sea SST and SIC data were extracted from the same NOAA OI dataset used to examine MHWs in the Bering Sea. The Air Temperature (AT) data was obtained from the ERA5 dataset which can be accessed through the C3S Climate Data Store (CDS).

The ERA5 dataset contains the latest significant improvements over its predecessors (Hersbach et al., 2020). In particular, energy budgets, fluxes and higher resolution data make the dataset useful for the study (Mayer et al., 2019). Estimates of ocean heat budgets in the ERA5 dataset are good on an annual mean basis, and the improved measurements of air temperatures by radiosonde and other sounding techniques have proved that the dataset has significant improvements on its former predecessors (Ingleby et al., 2016; Hersbach et al., 2020). The AO data was downloaded from the NOAA Climate Prediction Center (https://www.cpc.ncep.noaa.gov/). To be consistent with the observations and trends, the linear trends were removed before calculating the correlation coefficients.

3. Results

3.1. MHW mean states and trends

The number of MHW days is a sum of 40−50 and is seen in most parts of the Bering Sea (Figure 2a). The largest number is seen in the eastern Bering Sea and along the coasts of Bristol Bay in Alaska at approximately 58 MHW days. The smallest sum of 22 MHW days is seen along the coasts of Kamchatka Peninsula in Russia. The MHW frequencies show a wider range of values across the Bering Sea (Figure 2b). The map shows a higher number of MHW events in the western Bering Sea and Bering Strait. Moreover, 3 or more MHW events are found to occur in the regions of lower bathymetric depths in the Bering Sea. In comparison, lesser number of MHW events is observed in the eastern sectors of the sea. Long MHW durations are seen in the eastern Bering Sea at 25 days (Figure 2c), whereas most of the Bering Sea region shows an average of 15–20 days. The MHW mean intensities show a notable dipolar spatial pattern (Figure 2d). The MHW mean intensities of 1.8℃ are seen in the north with smaller variations along the bordering regions of East Russia and Alaska, and the lower values of 1–1.2℃ are seen in the southern sectors of the Bering Sea. The MHW maximum intensities show a similar spatial distribution as mean intensities but with relatively higher values (Figure 2e). Maximum MHW intensities appear in the north, ranging between 2.4–2.7℃ while the southern sectors of the Bering Sea are at values between 1.2–1.4 ℃.

Cumulative MHW intensities ranging from 50 to 65 °C days are seen in the eastern Bering Sea (Figure 2f). Other regions show lower values of 15–20 °C days.

Place Figure 2 here

Significant positive trends in MHW days are found across the entire area of the Bering Sea (Figure 3a). The highest decadal trends are found along the central and eastern sectors at 44 days/decade. A few regions in the central Bering Sea show comparatively larger values of 55–60 MHW days/decade. Increasing trends in MHW frequencies are also observed along the entire Bering Sea region except for the parts near the Aleutian Islands (Figure 3b). Comparatively higher trends of 2–3 MHW events/decade are observed in the west and along the coasts of the Russian Far East. Lower number of 1 MHW event per decade are seen in the Bering Strait and southern Bering Sea. Moreover, significant trends in MHW durations are noticed in most of the region except for the coastal areas near the Kamchatka Peninsula (Figure 3c). Longer periods of MHWs are seen in the eastern Bering Sea near the coasts of Aleutian Islands and Bristol Bay (Alaska). Significant trends in MHW mean intensities are noticed in the eastern Bering Sea (0.33 °C) and the Bering Strait (0.55 °C) (Figure 3d). Similar spatiotemporal trends are seen in maximum MHW intensities (Figure 3e). Higher values of 0.7–0.8°C/decade are observed in the north while the remaining sector shows lower values of 0.3–0.45 °C/decade. Cumulative MHW intensities are significantly higher in the coastal regions of southern Alaska with values ranging between 35 – 40 °C days/decade (Figure 3f).

Place Figure 3 here

3.2. Interrelationships between MHW characteristics and climate variables

Two MHW characteristics, namely MHW frequency and MHW days, are correlated to understand the connections between extreme marine events and regional climate factors. MHW frequencies have been increasing at the rate of 3 events per year for the time period 1990–2019 (Figure 4). Furthermore, the recent decade (2010–2019) shows the highest mean count of 4 while the first decade (1990–1999) shows the lowest mean count of 2. The highest MHW frequency is observed in 2017 at 7 MHW events. The MHW days have also been increasing at the rate of 3.92 (4 MHW days) per year for the same time period (Figure 4). While the recent decade (2010–2019) shows the highest mean MHW days of 93, the lowest number is seen in the first decade (1990–1999) at 21 mean MHW days. The largest number of MHW days was 172 days in 2018. Here we take into account the average of all MHWs that occur in the entire gridded dataset covering the Bering Sea region where "MHW days" refer to the total number of days in each year. We also find that in the first decade (1990–1999), MHW frequencies and days are at record highs in 1997, which is the same year a recorded MHW with maximum intensity of 5.1 °C, anomalously high atmospheric pressures near the eastern Bering Sea (particularly the Alaskan region) and seasonal changes in atmospheric circulation patterns in response to the El Niño impact on the ecosystems and climate regimes of the Bering Sea (Napp and Hunt, 2001). MHW frequencies and days (Figure 4) show a triple peaked pattern for the period of 30 years where each decade shows a bell-shaped pattern. It is interesting to note that these patterns (particularly 2000–2005 and 2007–2010) approximately reflect warm and cold events recorded in the eastern Bering Sea. Previous study has recorded warm and cold events in the southern Bering Sea compiling data from St. Pauls island (Alaska) for the periods 2001–2005 (warm) and 2007–2010 (cold) (Overland et al., 2012). Based on the climate record of six-year warm events followed by four-year cold events, the MHW frequencies tend to follow a similar temporal distribution.

Place Figure 4 here

Pearson correlation coefficients (r) were estimated to explore the underlying interrelationships between MHW characteristics (frequency and days) and climate variables (Table 2). Three of the climate variables, including Chukchi Sea SST/SIC and Alaska AT, show significant correlations (p-value less than 0.05) with both the MHW frequency and days; the other variables i.e. the Russian Arctic AT and AO do not show a significant correlation with either the MHW frequency or days.

In particular, Chukchi Sea SST shows an equally strong positive correlation, with similar r values when correlated with the MHW frequency (r = 0.70) and MHW days (r = 0.68). Seasonal behaviour is also depicted with positive correlations in the summers and winters. The Chukchi Sea SIC is the only climate variable showing a significant negative correlation with MHW frequencies (r = –0.67) and MHW days (r = –0.60). This indicates that the years with lower Chukchi Sea SIC witness more MHW events. The same is also true for MHW days. The Chukchi Sea SIC shows winter patterns with MHW frequencies (r = –0.55) and MHW days (r = –0.64), and shares a summer connection with only MHW frequencies. The correlation between Chukchi Sea SIC and MHW days in the winters is low (r = –0.30). Alaska AT shows a similar strength of correlation with the MHW frequency (r = 0.68) as Chukchi Sea SIC and SST, but shows a higher level of correlation (r = 0.74) with MHW days. This pattern is corroborated by Figure 2a which shows the largest number of MHW days close to the Alaskan Peninsula. There is a strong display of seasonal behaviour as well with significant correlations above 0.50. This seasonal behaviour can be attributed to the influence of the Aleutian Low pressure patterns, the North Pacific Oscillation (NPO) and the North Pacific Gyre Oscillation (NPGO). Previous studies have highlighted the variability in the Aleutian Low and NPO-NPGO coupling in response to winter SSTs in the north-eastern Pacific (Rodionov et al., 2007; Danielson et al., 2011). The Russian Arctic AT has no significant correlation with neither MHW frequency (r = 0.23) nor with MHW days (r = 0.21). A similar case can be made for the AO as well. Furthermore, the seasonally averaged AO also does not show significant correlations with MHW frequencies and MHW days.

Place Table 2 here

----

4. Discussion

4.1. Bering Sea MHW metrics and variability

In this study, the Bering Sea marine heatwave variability was examined on spatial and temporal scales. To better understand the air-sea interactions, the MHW metrics were also correlated with Arctic climate variables. MHW days are fairly equally-distributed throughout the Bering Sea although there is a larger average number of MHW days observed off the western coast of Alaska, with the number decreasing towards the south-west of the Bering Sea. Furthermore, certain areas such as the coasts of the Aleutian Islands and parts of central Bering Sea have a larger number of 58 days. Moreover, the southern coast of Alaska, Bristol Bay and the Aleutian Islands witness the largest number of MHW days (approximately 60–62 days). This is due to higher temperatures in southern Alaska as compared further north. In addition, air temperatures along the southern Alaskan coasts have been well correlated with teleconnections particularly the Pacific Decadal Oscillation (PDO) (Bieniek et al., 2011). This manifests that coastal MHW days–air temperature interactions are stronger and dependent on the PDO in the eastern Bering Sea. MHW frequencies are lower in the east and higher in the western Bering Sea. The east coast of the Russian Far East has a higher number of annual events (greater than 3) than the Alaskan coastline. Such spatial patterns exemplify the studies where MHW frequencies are greatly enhanced by SST re-emergence patterns associated with the thermocline circulation (Scannell et al., 2016).

An interesting observation can be made between the spatial distribution of MHW frequencies and durations. Here we find longer MHW durations and lower frequencies in the east Bering Sea, while the opposite is seen in the western sector. We reiterate that the MHW duration refers to the consecutive time period where the temperature exceeds the 90th percentile threshold. The spatial patterns observed in Figures 2a and 2c show higher number of MHW days and durations near the southern coasts of Alaska. This is due to the SST variability that exists in the Northern Pacific where higher SST anomalies are seen in the Eastern Bering Sea and further south along the western American coastline. This means that there are higher SSTs that persist for many days, implying a greater number of MHW days in this region. The spatiotemporal distribution of MHW mean and maximum intensities depicts higher values in the north as compared to the southern Bering Sea. The northern Bering Sea is generally characterised as having high-frequency dynamics and spatiotemporal variability as compared with the southern counterpart which shows gradual cold-to-warm transitions (Baker et al., 2020). While the Bering Sea shows relatively low MHW cumulative intensities, the regions off the western coasts of Alaska have higher values (greater than 45 °C days).

An interesting spatial pattern to note is the high MHW metrics (except frequencies) observed in the Eastern Bering Sea (and particularly near southern Alaska). A possibility does arise where the Aleutian Low in southern Alaska may be contributing to seasonal variability and trends in MHW metrics in the Bering Sea. A common spatial feature observed in all panels of Figure 2 is that the region of the Bering Sea south of 58° shows less MHW days and mean intensities. On the contrary, there is a greater number of MHW days, longer durations and higher intensities in the east and further north. From this perspective, the southern coasts of Alaska experience longer MHWs with higher intensities as compared to other regions in the Bering Sea. Such spatial characteristics can be influenced by North Pacific circulation patterns which have often dictated spatial trends in SSTs and seasonal teleconnections. The SST over the North Pacific bears similar resemblances to the higher latitudes (particularly Gulf of Alaska and the nearby south eastern Bering Sea region) (Yeo et al., 2014). Such resemblances have been attributed to the NPO which exerts a strong influence on the temperatures over central and north east Pacific Ocean. Therefore, the variability in MHW occurrences and intensities in the south eastern Being Sea are possibly driven by the NPO which in turn influences the oceanic NPGO of the Pacific Ocean. Furthermore, the coastal region of the Kamchatka Peninsula (Russia) experiences more frequent MHWs of very short durations as compared with other regions. Such shorter-duration MHWs may be due to a smaller influence of NPO and climate variability in the Pacific, although further studies are suggested in this aspect. Another explanation for the higher MHW metrics in the eastern Bering Sea is due to positive phases of the PDO, which consequently lead to warmer SSTs in the eastern Bering Sea and colder than normal temperatures in the west. Hence such teleconnections can act as potential drivers of longer and higher intensity MHWs in this region. Lastly, high surface heat fluxes and southeast-northwest advection currents have been linked with air temperatures and heat content in the central and southern sectors of the Bering Sea (Danielson et al., 2011). Therefore, our findings confirm the south-eastern Bering Sea as an MHW hotspot or an important MHW locale.

Higher positive trends in MHW days occur in the eastern Bering Sea and along the southern coasts of Alaska at greater than 50 days/decade. Similarly, positive trends in MHW durations are noticed in the same regions at 25–30 days/decade, indicating longer periods of MHWs. The trends in MHW frequencies are similar to mean states. A greater number of events per decade is seen along the coasts of Russian Far East while a smaller number is seen in the southern coasts of Alaska. Trends in MHW intensities also approximately mirror each other in spatial patterns. Significant mean, maximum and cumulative MHW intensity trends are noticed in the eastern sectors of the Bering Sea (Figures 3e-f). These trends are reflective of the mean SSTs in this region which are also considered as potential drivers of increasing MHW trends.

4.2. MHW temporal variations and connections with the Arctic climate

MHW events and annual days have been increasing since the 1990s with additional positive excursions also occurring throughout. Such positive excursions in MHW events occurred in the years 1996-1997, 2003, 2015 and 2017, while those in MHW days occurred in 1996, 2003 and 2018-2019. Anomalously low MHW frequency and MHW days occurred in 1999 and 2012 although there was a decreasing trend in the years preceding both of these lows. In these multiyear periods with increasing MHW trends (such as 2000-2005 and 2014-2018), sea ice was at its minimum in the southern Bering shelves. Certain oceanographic conditions can draw clues to the MHW metrics in the Bering Sea. The years from 2016 to 2019 show a lack of sea ice in the northern and south-eastern Bering Sea shelves and no cold pools in the summers. During the same years, we find a larger number of MHW days (mean of 140 days) and MHW events (mean of 6 events). The years from 1990 to 2015 witness an average of 44 annual MHW days and 4 MHW events. Therefore, warmer years serve as important signs and precursors for extreme ocean temperature anomalies.

Positive correlation in most of the climate variables indicate that MHW frequencies and the number of MHW days are greatly influenced by Arctic climate. The Chukchi Sea SST with a high positive correlation hints that the Bering Sea heatwave frequencies and number of days are strongly related to it. It implies that the Bering Sea MHW metrics may be affected by interannual variability in the SST further north. The opposite is seen with ice concentration in the adjoining sea. The Chukchi Sea SIC shows a negative correlation with the MHW metrics, i.e. a decrease in sea ice can lead to more MHW days and greater counts per year. The recent decades that show increasing MHW frequencies and the number of MHW days are attributed to the decreasing sea ice thickness, huge loss in sea ice and reduction of ice cover in the Pacific Arctic. Climate simulations have hinted that the reduction in ice concentration has further influenced cryosphere dynamics in the Pacific

Arctic region (Baker et al., 2020). Hence, this further implicates a decreasing Chukchi SIC with increasing MHW frequencies and days. Moreover, a high positive correlation with the Alaskan AT proves that MHW annual counts and days in the Bering Sea are greatly influenced by air temperatures in Alaska. Lastly, no significant correlation of MHW metrics with the Russian Arctic AT and AO states that these variables have negligible or no influence on MHWs in the Bering Sea. It is worth mentioning the relationships between AO, Alaskan AT and Bering Sea MHW metrics. While it is proven that AO is negatively correlated with Alaskan temperatures, the Bering Sea MHW frequency and annual days are not influenced by AO, which brings a distinct characteristic to this relationship. The above results bring us to the important question: does the Arctic climate influence the neighbouring high latitude circulation and atmospheric patterns?

Our study provides evidence supporting the theory that a connection is present between Chukchi Sea SST, SIC and the Alaskan air temperatures on Bering Sea extremes – marine heatwaves. Furthermore, the long-period analysis of this study provides a better understanding of the relationship between the Bering Sea extremes and the Chukchi Sea and Alaskan climates. How is the theorised relationship defined? Our observations conclude that the Chukchi Sea SST and Alaskan temperatures have a positive correlation with Bering Sea MHW frequencies and annual MHW days, while the Chukchi SIC presents an inverse relationship with the aforementioned MHW metrics. In order to postulate a few theses, we follow the hypothesis by Francis and Vavrus (2012) which states that Arctic amplification and subsequent warming may cause persistent weather patterns and extreme weather in near mid-latitude environments. According to the Rossby wave theory, slower moving circulation systems which are caused by reduced poleward gradients in the 1000-500 hPa thicknesses tend to weaken the upper-zonal flow. While sea ice loss and subsequent transfer of heat energy from the ocean into the atmosphere are prominent in the autumn and winters, the enhanced warming over Alaska leading to snow melt and heating of the Chukchi shelf is a common occurrence in the summers. Decrease in sea ice can also lead to greater ocean temperatures due to the exposure of open waters. Such a prolongation of weather i.e. increases in Chukchi sea temperatures, reduced sea ice loss and high Alaskan temperatures can account for extreme weather conditions – marine heatwaves in the Bering Sea. This statement is supported by the anomalous warming event of 2015-2016 in the Bering Sea which was caused by excessive heat content in the Gulf of Alaska and higher temperatures along the Alaskan coasts.

The slow-moving weather patterns can be caused by the enhanced 500-hPa ridging (ridge elongation due to large increases in 500-hPa heights), and such patterns have also led to extreme weather and heatwaves across Europe in recent summers (Jaeger and Seneviratne, 2011). Questions arise from the above concluded relationship – Can the Chukchi Sea climate alone lead to Bering Sea MHWs? Do the Alaskan air temperatures solely contribute to the Bering Sea MHWs? As shown in Table 2, it is evident that the Alaskan AT has higher r values in correlation with the MHW metric. However, future development can bring about more inferences from the same. Our theses can be summed up in the flowchart shown in Figure 5. As mentioned previously, the correlations were performed after removing the linear trends. Slightly higher r values can be found if the mean is removed. Also similar results can be obtained if the data is not detrended before the correlations are performed.

Place Figure 5 here

----

5. Summary and Conclusions

This paper explores the spatiotemporal evolution characteristics and occurrence mechanisms of MHWs in the Bering Sea with emphasis on different key metrics as defined by Hobday et al. (2016). Different metrics are analysed on spatiotemporal scales, which provides an in-depth analysis of geographic patterns of extremes in the Bering Sea. In addition, MHW frequencies and the number of MHW days are correlated with different climate variables, further disclosing the underlying connections between the air and sea properties. In addition to examining relationships between MHWs and climate variables, this paper offers a glimpse of Arctic cryosphere influences on neighbouring seas at lower latitudes i.e. the Bering Sea.

While a number of studies in understanding marine extremes have been conducted in the recent past, it is useful to note that the latest definition of MHWs has been used as a key basis in this study. Further studies based on model experiments would be undertaken to fill in the gaps existing in the marine heatwave knowledge, particularly on physical, ecological impacts and geographical connections. Additional in-situ analyses and laboratory experiments are also beneficial in understanding MHW impacts on ecosystems, communities, and socioeconomic services.

Acknowledgments

This research was supported by the National Natural Science Foundation of China (Grant No. 51809223) and the Hong Kong Research Grants Council Early Career Scheme (Grant No.

PP5Z). We would like to express our sincere gratitude to the editor and anonymous reviewers for their constructive comments and suggestions.

References

Baker, M.R., Kivva, K.K., Pisareva, M.N., Watson, J.T., Selivanova, J., 2020. Shifts in the physical environment in the Pacific Arctic and implications for ecological timing and conditions. Deep Sea Research Part II: Topical Studies in Oceanography, 104802. https://doi.org/10.1016/j.dsr2.2020.104802.

Banzon, V., Smith, T.M., Steele, M., Huang, B., Zhang, H., 2020. Improved Estimation of Proxy Sea Surface Temperature in the Arctic. J. Atmos. Oceanic Technol. 37, 341–349. https://doi.org/10.1175/JTECH-D-19-0177.1.

Bieniek, P.A., Bhatt, U.S., Thoman, R.L., 2011. Climate Divisions for Alaska Based on Objective Methods. J. Appl. Meteor. Climatol., 51, 1276–1289. https://doi.org/10.1175/JAMC-D-11-0168.1.

Blackport, R., Screen, J.A., 2020. Insignificant effect of Arctic amplification on the amplitude of midlatitude atmospheric waves. Science Advances, 6. https://doi.org/10.1126/sciadv.aay2880.

Bond, N.A., Cronin, M.F., Freeland, H., Mantua, N., 2015. Causes and impacts of the 2014 warm anomaly in the NE Pacific. Geophys. Res. Lett. 42, 3414-3420. https://doi.org/10.1002/2015GL063306.

Carvalho, K.S., Wang, S., 2020. Sea surface temperature variability in the Arctic Ocean and its marginal seas in a changing climate: Patterns and mechanisms. Global Plan. Change 193, 103265. https://doi.org/10.1016/j.gloplacha.2020.103265.

Danielson, S., Curchitser, E., Hedstrom, K., Weingartner, T., Stabeno, P. 2011. On ocean and sea ice modes of variability in the Bering Sea. J. Geophys. Res. 116, C12034. https://doi:10.1029/2011JC007389.

Fischer, E.M., Lawrence, D.M., Sanderson, B.M., 2011. Quantifying uncertainties in projections of extremes – a perturbed land surface parameter experiment. Clim. Dyn. 37 (7-8), 1381-1398. https://doi.org/10.1007/s00382-010-0915-y.

Francis, J.A., 2017. Why are Arctic linkages to extreme weather still up in the air?. Bull. Amer. Meteor. Soc. 98, 2551-2557. https://doi.org/10.1175/BAMS-D-17-0006.1.

Francis, J.A., Vavrus, S.J., 2012. Evidence linking Arctic amplification to extreme weather in mid-latitudes. Geophys. Res. Lett., 39, L06801. https://doi:10.1029/2012GL051000.

Frölicher, T.L., Laufkötter, C., 2018. Emerging risks from marine heat waves. Nat. Commun. 9**,** 650. https://doi.org/10.1038/s41467-018-03163-6

Hersbach, H., Bell, B., Berrisford, P., et al., 2020. The ERA5 global reanalysis. Quarterly Journal of the Royal Meteorological Society, 1-51. https://doi.org/10.1002/qj.3803.

Hobday, A.J., Alexander, L.V., Perkins, S.E., et al., 2016. A hierarchical approach to defining marine heatwaves. Progress in Oceanography 141, 227-238. https://doi.org/10.1016/j.pocean.2015.12.014

Ingleby, B., Pauley, P., Kats, A., Ator, J., Keyser, D., Doerenbecher, A., Fucile, E., Hasegawa, J., Toyoda, E., Kleinert, T., Qu, W., St. James, J., Tennant, W., & Weedon, R.

(2016). Progress toward High-Resolution, Real-Time Radiosonde Reports. Bulletin of the American Meteorological Society, 97(11), 2149-2161. https://doi.org/10.1175/BAMS-D-15-00169.1.

Jaeger, E.B., Seneviratne, S.I., 2011. Impact of soil moisture-atmosphere coupling on European climate extremes and trends in a regional climate model. Clim. Dyn., 36, 1919 – 1939. https://doi.org/10.1007/s00382-010-0780-8.

Jentsch, A., Kreyling, J., Beierkuhnlein, C., 2007. A new generation of climate-change experiments: events, not trends. Front. Ecol. Environ. 5 (6), 315-324. https://doi.org/10.1890/1540-9295(2007)5[365:ANGOCE]2.0.CO;2.

Kretschmer, M., Coumou, D., Agel, L., Barlow, M., Tziperman, E., Cohen, J., 2018. More-Persistent Weak Stratospheric Polar Vortex States Linked to Cold Extremes. Bull. Amer. Meteor. Soc. 99, 49–60. https://doi.org/10.1175/BAMS-D-16-0259.1.

Mayer, M., Tietsche, S., Haimberger, L., Tsubouchi, T., Mayer, J., Zuo, H., 2019. An Improved Estimate of the Coupled Arctic Energy Budget. J. Climate, 32, 7915–7934. https://doi.org/10.1175/JCLI-D-19-0233.1.

Meehl, G.A., Tebaldi, C., 2004. More intense, more frequent, and longer lasting heat waves in the 21st century. Science 305 (5686), 994-997. https:// doi.org/10.1126/science.1098704.

Mills, K.E., Pershing, A.J., Brown, C.J., Chen, Y., Chiang, F-S., Holland, D.S., Lehuta, S., Nye, J.A., Sun, J.C., Thomas, A.C., Wahle. R.A., 2013. Fisheries management in a changing climate: Lessons from the 2012 ocean heat wave in the Northwest Atlantic. Oceanography 26 (2),191–195. https://doi.org/10.5670/oceanog.2013.27.

Napp, J.M., Hunt, G.L., 2001. Anomalous conditions in the south-eastern Bering Sea 1997: linkages among climate, weather, ocean, and Biology. Fish. Oceano. 10, 61-68. https://doi.org/10.1046/j.1365-2419.2001.00155.x.

Niebauer, H. J., 1988. Effects of El Nino-Southern Oscillation and North Pacific weather patterns on interannual variability in the subarctic Bering Sea. J. Geophys. Res., 93(C5), 5051– 5068, https://doi:10.1029/JC093iC05p05051.

Olita, A., Sorgente, R., Natale, S., Gaberšek, S., Ribotti, A., Bonanno, A., Patti, B., 2007. Effects of the 2003 European heatwave on the Central Mediterranean Sea: surface fluxes and the dynamical response. Ocean Sci. 3, 273-289. https://doi.org/10.5194/os-3-273-2007.

Oliver, E.C.J., Benthuysen, J.A., Bindoff, N.L., Hobday, A.J., Holbrook, N.J., Mundy, C.N., Perkins-Kirkpatrick, S.E., 2017. The unprecedented 2015/16 Tasman Sea marine heatwave. Nat. Commun. 8, 16101. https://doi.org/10.1038/ncomms16101.

Overland, J. E., Wang, M., Wood, K.R., Percival, D.B., Bond, N.A., 2012. Recent Bering Sea warm and cold events in a 95-year context. Deep-Sea Research II, 65-70, 6-13. https://doi.org/10.1016/j.dsr2.2012.02.013.

Perkins, S.E., Alexander, L.V., 2013. On the measurement of heatwaves. J. Clim. 26 (13), 4500-4517. https://doi.org/10.1175/JCLI-D-12-00383.1.

Reynolds, R.W., Smith, T.M., Liu, C., Chelton, D.B., Casey, K.S., Schlax, M.G., 2007. Daily High-Resolution-Blended Analyses for Sea Surface Temperature. J. Clim., 20, 5473-5496. https://doi.org/10.1175/2007JCLI1824.1.

Rodionov, S.N., Bond, N.A., Overland, J.E., 2007. The Aleutian Low, storm tracks, and winter climate variability in the Bering Sea. Deep Sea Research Part II: Topical Studies in Oceanography 23-26, 2560-2577. https://doi.org/10.1016/j.dsr2.2007.08.002.

Ruela, R., Sousa, M.C., deCastro, M., Dias, J.M., 2020. Global and regional evolution of sea surface temperature under climate change. Global Planet. Change 190, 103190. https://doi.org/10.1016/j.gloplacha.2020.103190.

Scannell, H., Pershing, A.J., Alexander, M.A., Thomas, A.C., Mills, K.E., 2016. Frequency of marine heatwaves in the North Atlantic and North Pacific since 1950. Geophys. Res. Lett. 43, 2069-2076. https://doi.org/10.1002/2015GL067308.

Screen, J.A., 2014. Arctic amplification decreases temperature variance in northern mid-to high-latitudes. Nat. Clim. Chang., 4, 577-582. https://doi.org/10.1038/nclimate2268.

Selig, E.R., Casey, K.S., Bruno, J.F., 2010. New insights into global patterns of ocean temperature anomalies: implications for coral reef health and management. Global Ecology and Biogeography 19, 397-411. https://doi.org/10.1111/j.1466-8238.2009.00522.x.

Smale, D.A., Wernberg, T., Oliver, E.C.J., et al., 2019. Marine heatwaves threaten global biodiversity and the provision of ecosystem services. Nat. Clim. Chang. 9, 306-312. https://doi.org/10.1038/s41558-019-0412-1.

Smith, C.A., Compo, G.P., Hooper, D.K., 2014. Web-Based Reanalysis Intercomparison Tools (WRIT) for Analysis and Comparison of Reanalyses and Other Datasets. Bulletin of the American Meteorological Society, 95(11), 1671-1678. https://doi.org/10.1175/BAMS-D-13-00192.1.

Sparnocchia, S., Schiano, M.E., Picco, P., Bozzano, R., Cappelletti, A., 2006. The anomalous warming of summer 2003 in the surface layer of the Central Ligurian Sea (Western Mediterranean). Ann. Geophys. 24, 443-452. https://doi.org/10.5194/angeo-24-443-2006.

Wang, M., Overland, J.E., Bond, N.A., 2010. Climate projections for selected large marine ecosystems. Journal of Marine Systems, 79, 258-266. https://doi.org/10.1016/j.jmarsys.2008.11.028.

Wang, S., Zhu, J., 2020. Amplified or exaggerated changes in perceived temperature extremes under global warming. Clim. Dyn. 54, 117-127. https://doi.org/10.1007/s00382-019-04994-9.

Wood, K.R., Bond, N.A., Danielson, S. L., Overland, J.E., Salo, S.A., Stabeno, P.J., Whitefield, J., 2015. A decade of environmental change in the Pacific Arctic region. Progress in Oceanography 136, 12-31. http://dx.doi.org/10.1016/j.pocean.2015.05.005.

Woodgate, R.A., Weingartner, T.J., Lindsay, R., 2012. Observed increases in Bering Strait oceanic fluxes from the Pacific to the Arctic from 2001 to 2011 and their impacts on the Arctic Ocean water column. Geophys. Res. Lett. 39, L24603. https://doi.org/10.1029/2012GL054092.

Yeo, S., Kim, K., Yeh, S., Kim, B., Shim, T., Jhun, J., 2014. Recent climate variation in the Bering and Chukchi Seas and its linkages to large-scale circulation in the Pacific. Climate Dynamics. 42, 2423-2437. https://doi.org/10.1007/s00382-013-2042-z.

List of Figure Captions

Figure 1. Map of the study area including the Bering Sea and the Arctic–North Pacific sector (left). The coloured boxes indicate the Arctic regions neighbouring the Bering Sea (right). Climate variables of these Arctic regions are correlated with MHW characteristics of the Bering Sea: Orange – Russian Arctic region, Pink – Alaska, and Black – Chukchi Sea (refer to section 2.3 for further details).

Figure 2. Annual mean states of MHW metrics in the Bering Sea.

Figure 3. Trends in MHW metrics in the Bering Sea. The stippled areas indicate significant trends where p-values are less than 0.05.

Figure 4. The MHW frequencies (blue bars) and annual MHW days (green bars) for the time period 1990 – 2019.

Figure 5. Flowchart depicting a combination of Arctic variables that have an influence on the Bering Sea MHWs. Here, an increase in Chukchi Sea SST and Alaskan AT coupled with a decrease in Chukchi Sea SIC is theorised as a possible cause of MHWs in the Bering Sea.

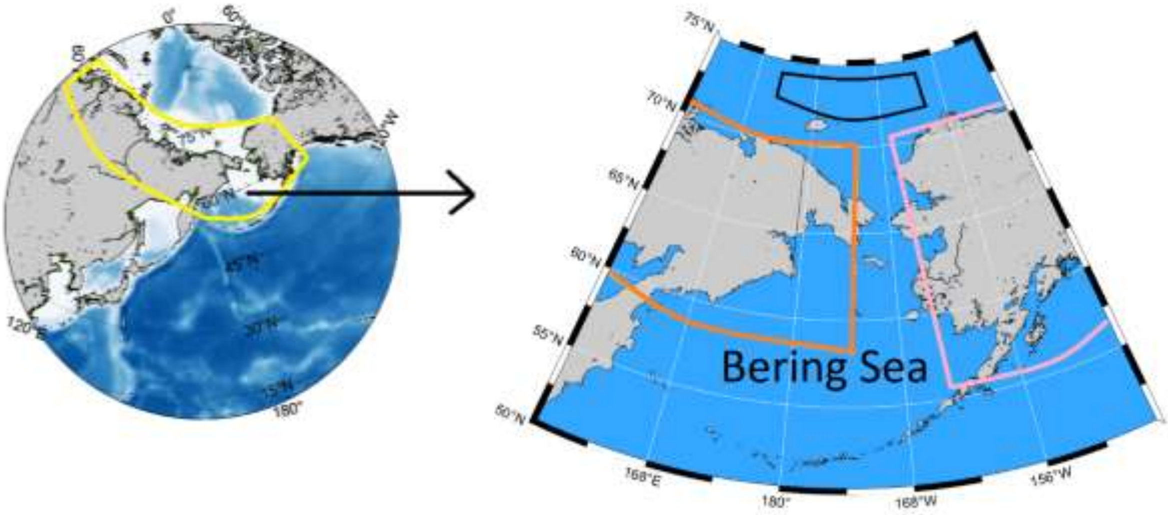

Figure 1. Map of the study area including the Bering Sea and the Arctic–North Pacific sector (left). The coloured boxes indicate the Arctic regions neighbouring the Bering Sea (right). Climate variables of these Arctic regions are correlated with MHW characteristics of the Bering Sea: Orange – Russian Arctic region, Pink – Alaska, and Black – Chukchi Sea (refer to section 2.3 for further details).

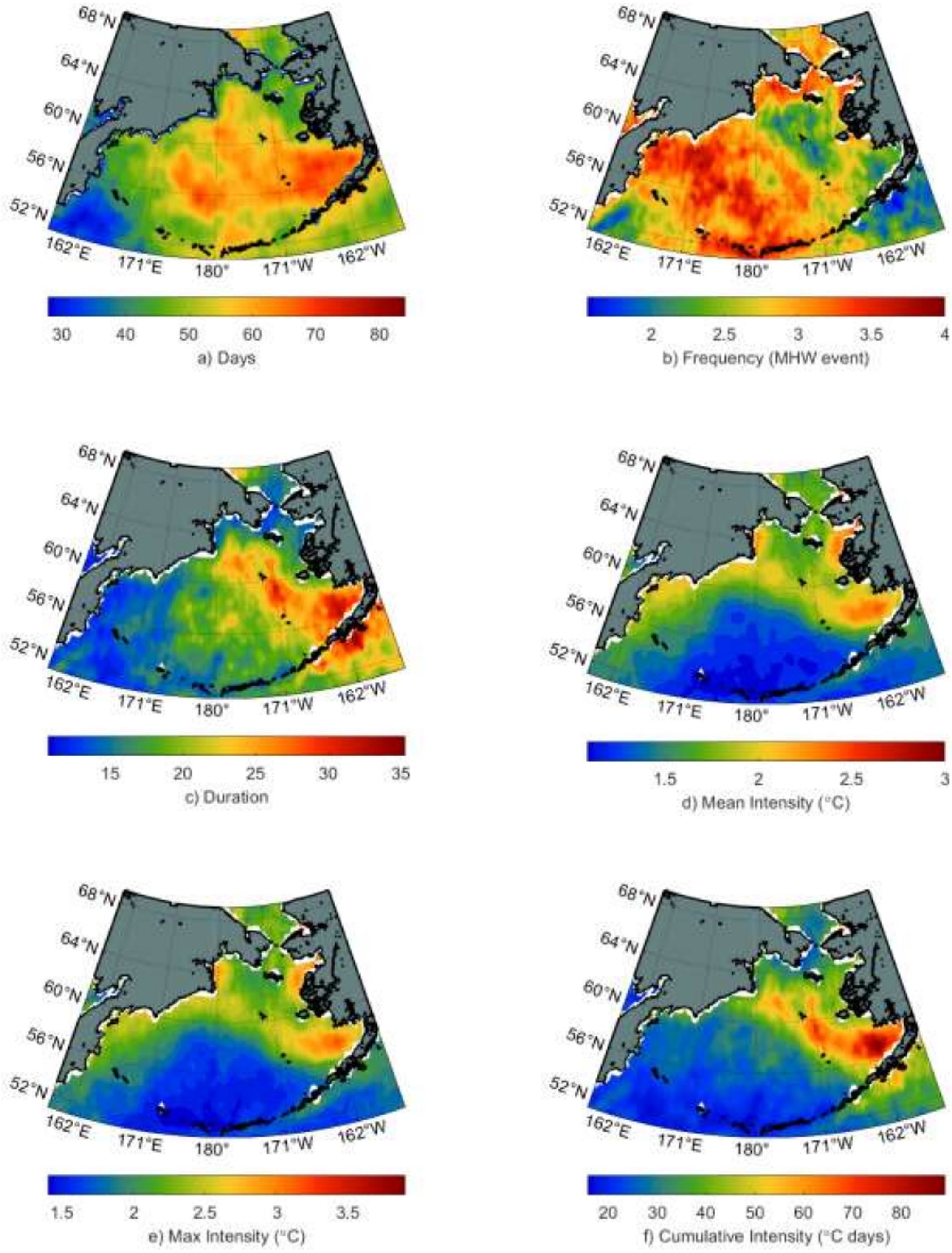

Figure 2. Annual mean states of MHW metrics in the Bering Sea.

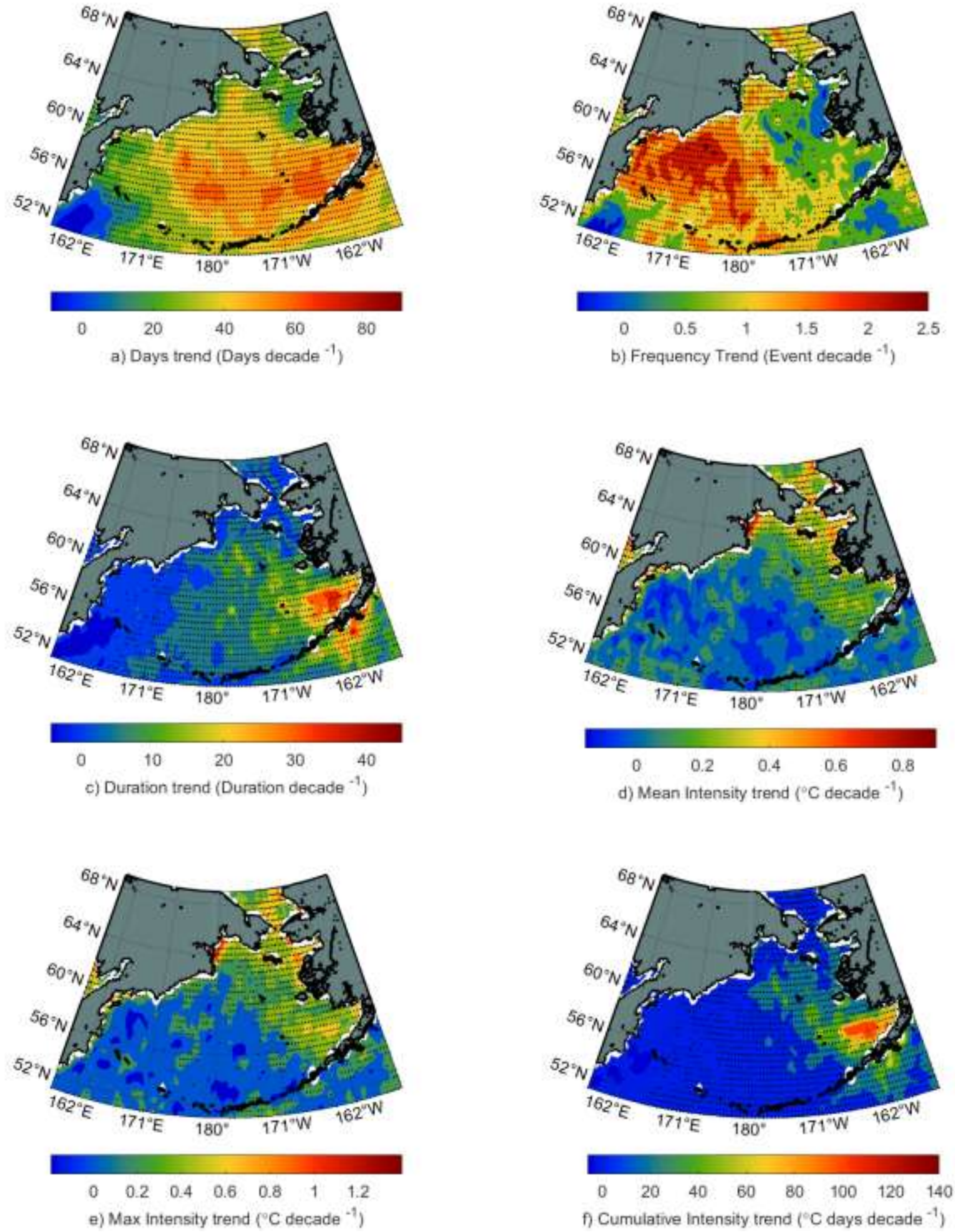

Figure 3. Trends in MHW metrics in the Bering Sea. The stippled areas indicate significant trends where p-values are less than 0.05.

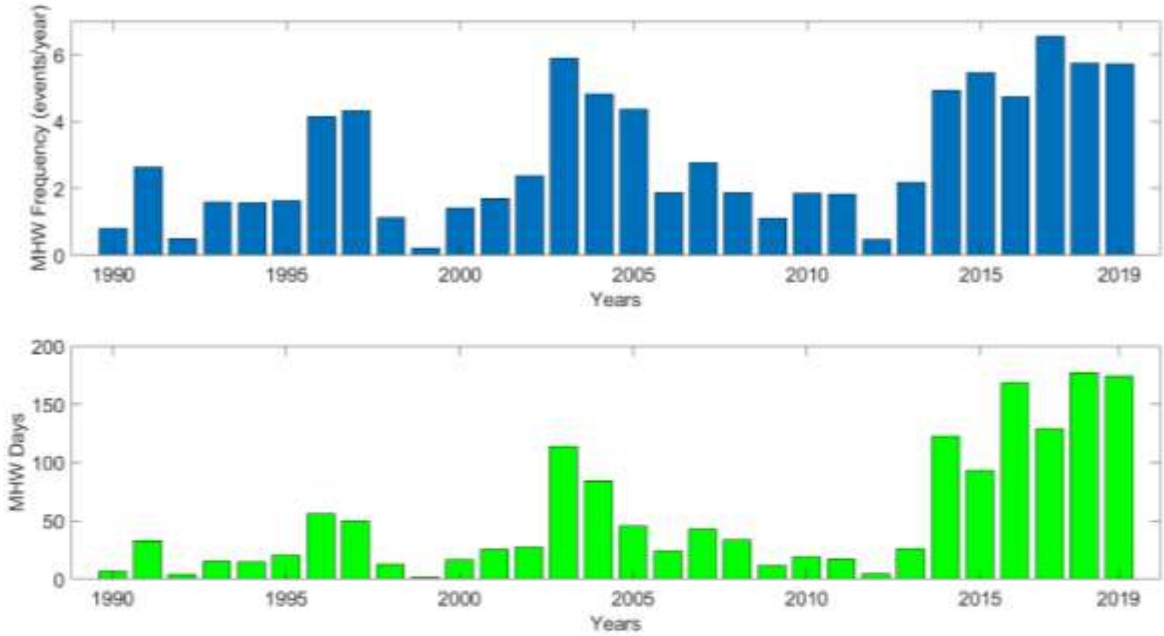

Figure 4. The MHW frequencies (blue bars) and annual MHW days (green bars) for the time period 1990–2019.

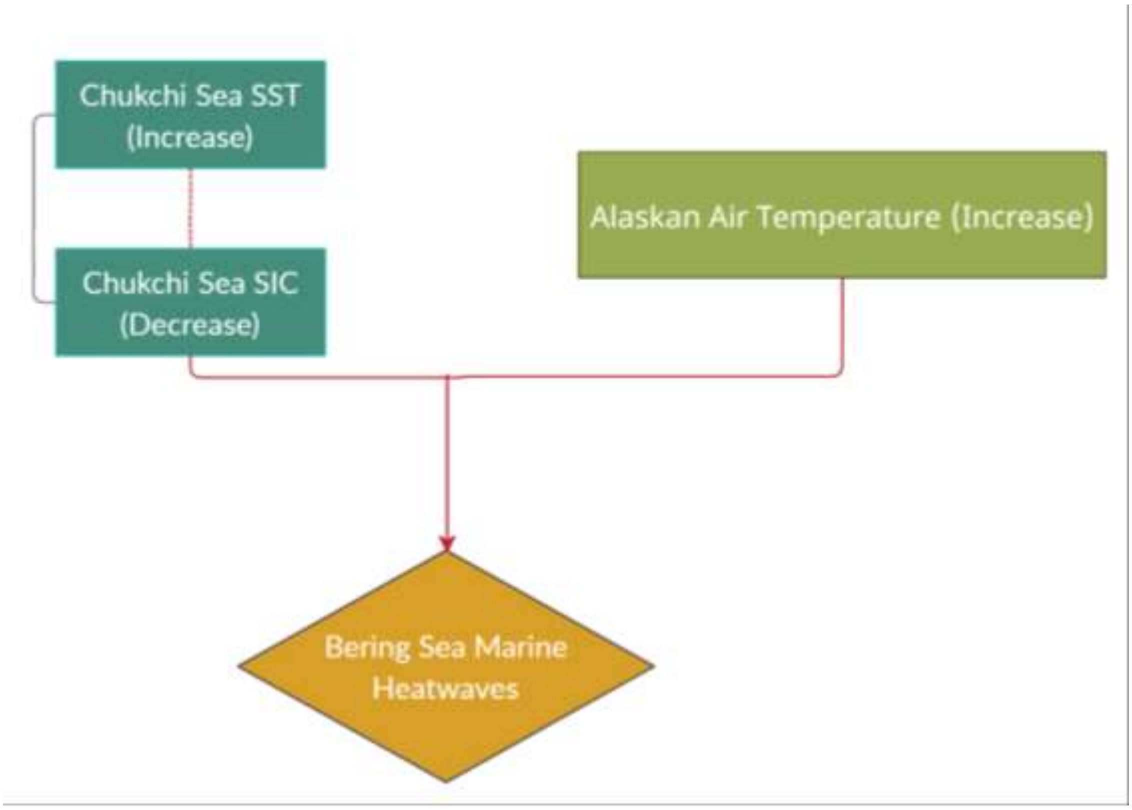

Figure 5. Flowchart depicting a combination of Arctic variables that have an influence on the Bering Sea MHWs. Here, an increase in Chukchi Sea SST and Alaskan AT coupled with a decrease in Chukchi Sea SIC is theorised as a possible cause of MHWs in the Bering Sea.

List of Table Captions

Table 1. Classification of marine heatwave (MHW) metrics, units and descriptions, after Hobday et al. (2016).

Table 2. Correlation statistics derived to reveal the interrelationships between MHW characteristics (frequency and days) and climate variables of the Arctic region. The correlations with p-values less than 0.05 are statistically significant (see text for further details).

Table 1. Classification of marine heatwave (MHW) metrics, units and descriptions, after Hobday et al. (2016).

Metric	Description	Unit
Duration	Time period between the start and end of MHW	days
Maximum Intensity	Maximum temperature anomaly that exceeds the threshold	℃
Mean Intensity	Mean temperature anomaly during the MHW event	℃
Cumulative Intensity	Integral of the temperature anomaly above the climatology	℃ days

Table 2. Correlation statistics derived to reveal the interrelationships between MHW characteristics (frequency and days) and climate variables of the Arctic region. The correlations with p-values less than 0.05 are statistically significant (see text for further details).

Climate Variable	MHW Frequency			MHW Days		
	Correlation coefficient (r)			Correlation coefficient (r)		
	Annual	Summer	Winter	Annual	Summer	Winter
Chukchi Sea SST	0.70	0.64	0.60	0.68	0.50	0.65
Chukchi Sea SIC	-0.67	-0.54	-0.55	-0.61	-0.30	-0.64
Alaska AT	0.68	0.65	0.58	0.75	0.64	0.58
Russian Arctic AT	0.23	-0.03	0.11	0.21	0.10	0.19
Arctic Oscillation (AO)	0.06	0.10	0.07	0.12	0.20	0.10